NTNU

# Student Project

*Group members:* 10016, 10044, 10052, and 10055

**Abstract**

Maxwell's equations are introduced and a numerical method for obtaining an approximate solution to these equations is presented. The stability and consistency is discussed, and the convergence of the method is asserted. The resulting numerical method, commonly known as the "Yee method" or "Finite Difference Time Domain Method", is shown to behave nicely and approach analytical reference solutions as the temporal and spatial stepsizes decrease. The convergence in space is shown to be of order 2, while the convergence in time is shown to be of order 1. The latter of these results is not in line with what would be expected from the theory and is therefore discussed in more detail.

## Introduction

Maxwell's equations are the fundamental equations of electromagnetism and model the behaviour of electromagnetic waves as they move through time and space. The equations simplify considerably for free space with no charge- or current densities, which is what will be considered here. This leads to equations where the derivative of one field component can be expressed in terms of the derivative of the other field's components. The derivatives are approximated by the use of central differences and combined into a discretization scheme known as the "Yee method". Several different problem instances will be investigated with the method.

## Theory

### 2.1 Maxwell's equations

Maxwell's equations in three dimensions, using Gaussian units [3], are

$$\frac{\partial \mathbf{B}}{\partial t} = -c\nabla\times\mathbf{E}, \tag{1a}$$

$$\left(4\pi\mathbf{J} + \frac{\partial \mathbf{E}}{\partial t}\right) = c\nabla\times\mathbf{B}, \tag{1b}$$

$$\nabla\cdot\mathbf{B} = 0, \tag{1c}$$

$$\nabla\cdot\mathbf{E} = 4\pi\rho. \tag{1d}$$

We will make several simplifying assumptions regarding these equations. Firstly, it can be shown that as long as (1c) and (1d) are satisfied for any $t = t_0$, it will be satisfied for all other $t$ [2]. The numerical scheme will only be concerned with (1a) and (1b), and assume that (1c) and (1d) are satisfied for the chosen initial conditions. We also assume there to be zero electric charge ($\rho$) and current ($\mathbf{J}$) density. This yields a simplified system of equations,

$$\frac{\partial B_x}{\partial t} = -c\left(\frac{\partial E_z}{\partial y} - \frac{\partial E_y}{\partial z}\right) \tag{2a}$$

$$\frac{\partial B_y}{\partial t} = -c\left(\frac{\partial E_x}{\partial z} - \frac{\partial E_z}{\partial x}\right) \tag{2b}$$

$$\frac{\partial B_z}{\partial t} = -c\left(\frac{\partial E_y}{\partial x} - \frac{\partial E_x}{\partial y}\right) \tag{2c}$$

$$\frac{\partial E_x}{\partial t} = c\left(\frac{\partial B_z}{\partial y} - \frac{\partial B_y}{\partial z}\right) \tag{2d}$$

$$\frac{\partial E_y}{\partial t} = c\left(\frac{\partial B_x}{\partial z} - \frac{\partial B_z}{\partial x}\right) \tag{2e}$$

$$\frac{\partial E_z}{\partial t} = c\left(\frac{\partial B_y}{\partial x} - \frac{\partial B_x}{\partial y}\right) \tag{2f}$$

The equations can be simplified to the one-dimensional case by assuming that the two fields are functions of only $x$, and choosing the $z$-axis to be coinciding with the electric field component. This gives

$$-\frac{\partial \mathbf{B}}{\partial t} = c \begin{vmatrix} \mathbf{e}_x & \mathbf{e}_y & \mathbf{e}_z \\ \frac{\partial}{\partial x} & 0 & 0 \\ 0 & 0 & E_z \end{vmatrix} = -c\frac{\partial E_z}{\partial x}\mathbf{e}_y, \tag{3a}$$

$$\frac{\partial \mathbf{E}}{\partial t} = c \begin{vmatrix} \mathbf{e}_x & \mathbf{e}_y & \mathbf{e}_z \\ \frac{\partial}{\partial x} & 0 & 0 \\ 0 & B_y & 0 \end{vmatrix} = c\frac{\partial B_y}{\partial x}\mathbf{e}_z, \tag{3b}$$

which simplifies to

$$\frac{\partial B_y}{\partial t} = c\frac{\partial E_z}{\partial x}, \tag{4a}$$

$$\frac{\partial E_z}{\partial t} = c\frac{\partial B_y}{\partial x}. \tag{4b}$$

## 2.2 Yee's discretization scheme

One can observe that the time derivative of each field is entirely determined by the spatial derivatives of the other field. This fact is utilized in the numerical scheme, as it is only necessary to know the value of one of the fields when calculating the other. The calculated magnetic field nodes are offset by one half time-step relative to the electric field nodes, never calculating both fields at the exact same time. This saves a factor of two in computational effort.

Using second order approximations of the partial derivatives in time and space, one obtains the following update equations:

$$B_y\Big|_{m+\frac{1}{2}}^{n+\frac{1}{2}} = B_y\Big|_{m+\frac{1}{2}}^{n-\frac{1}{2}} + cp\left(E_z\Big|_{m+1}^{n} - E_z\Big|_{m-1}^{n}\right), \tag{5a}$$

$$E_z\Big|_{m}^{n+1} = E_z\Big|_{m}^{n} + cp\left(B_y\Big|_{m+\frac{1}{2}}^{n+\frac{1}{2}} - B_y\Big|_{m-\frac{1}{2}}^{n+\frac{1}{2}}\right). \tag{5b}$$

The scheme was first proposed by Yee [7] in 1966, and a grid explaining the scheme is shown in figure 1.

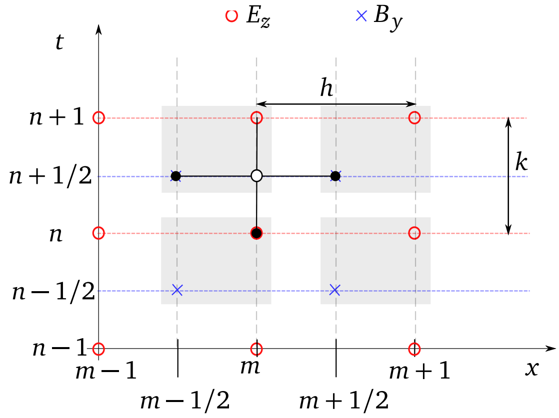


**Figure 1:** Yee's discretization scheme in one dimension. Each grey rectangle is one basic grid unit. Update equation (5b) for the electric field is visualized.

The same approach can be applied for the three-dimensional case, where equations (2a - 2c) are discretized in order to update the magnetic field, and likewise for equations (2d - 2f) for the electric field. This gives the following update equations

$$B_x\Big|_{i,j+\frac{1}{2},k+\frac{1}{2}}^{n+\frac{1}{2}} = B_x\Big|_{i,j+\frac{1}{2},k+\frac{1}{2}}^{n-\frac{1}{2}} - cp\left(E_z\Big|_{i,j+1,k+\frac{1}{2}}^{n} - E_z\Big|_{i,j,k+\frac{1}{2}}^{n} - \left(E_y\Big|_{i,j+\frac{1}{2},k+1}^{n} - E_y\Big|_{i,j+\frac{1}{2},k}^{n}\right)\right), \tag{6a}$$

$$B_y\Big|_{i+\frac{1}{2},j,k+\frac{1}{2}}^{n+\frac{1}{2}} = B_y\Big|_{i+\frac{1}{2},j,k+\frac{1}{2}}^{n-\frac{1}{2}} - cp\left(E_x\Big|_{i+\frac{1}{2},j,k+1}^{n} - E_x\Big|_{i+\frac{1}{2},j,k}^{n} - \left(E_z\Big|_{i+1,j,k+\frac{1}{2}}^{n} - E_z\Big|_{i,j,k+\frac{1}{2}}^{n}\right)\right), \tag{6b}$$

$$B_z\Big|_{i+\frac{1}{2},j+\frac{1}{2},k}^{n+\frac{1}{2}} = B_z\Big|_{i+\frac{1}{2},j+\frac{1}{2},k}^{n-\frac{1}{2}} - cp\left(E_y\Big|_{i+1,j+\frac{1}{2},k}^{n} - E_y\Big|_{i,j+\frac{1}{2},k}^{n} - \left(E_x\Big|_{i+\frac{1}{2},j+1,k}^{n} - E_x\Big|_{i+\frac{1}{2},j,k}^{n}\right)\right), \tag{6c}$$

$$E_x\Big|_{i+\frac{1}{2},j,k}^{n+1} = E_x\Big|_{i+\frac{1}{2},j,k}^{n} + cp\left(B_z\Big|_{i+\frac{1}{2},j+\frac{1}{2},k}^{n+\frac{1}{2}} - B_z\Big|_{i+\frac{1}{2},j-\frac{1}{2},k}^{n+\frac{1}{2}} - \left(B_y\Big|_{i+\frac{1}{2},j,k+\frac{1}{2}}^{n+\frac{1}{2}} - B_y\Big|_{i+\frac{1}{2},j,k-\frac{1}{2}}^{n+\frac{1}{2}}\right)\right), \tag{6d}$$

$$E_y\Big|_{i,j+\frac{1}{2},k}^{n+1} = E_y\Big|_{i,j+\frac{1}{2},k}^{n} + cp\left(B_x\Big|_{i,j+\frac{1}{2},k+\frac{1}{2}}^{n+\frac{1}{2}} - B_x\Big|_{i,j+\frac{1}{2},k-\frac{1}{2}}^{n+\frac{1}{2}} - \left(B_z\Big|_{i+\frac{1}{2},j+\frac{1}{2},k}^{n+\frac{1}{2}} - B_z\Big|_{i-\frac{1}{2},j+\frac{1}{2},k}^{n+\frac{1}{2}}\right)\right), \tag{6e}$$

$$E_z\Big|_{i,j,k+\frac{1}{2}}^{n+1} = E_z\Big|_{i,j,k+\frac{1}{2}}^{n} + cp\left(B_y\Big|_{i+\frac{1}{2},j,k+\frac{1}{2}}^{n+\frac{1}{2}} - B_y\Big|_{i-\frac{1}{2},j,k+\frac{1}{2}}^{n+\frac{1}{2}} - \left(B_x\Big|_{i,j+\frac{1}{2},k+\frac{1}{2}}^{n+\frac{1}{2}} - B_x\Big|_{i,j-\frac{1}{2},k+\frac{1}{2}}^{n+\frac{1}{2}}\right)\right). \tag{6f}$$

The spatial nodes used by the scheme are shown visually in figure 2a.

For 8 spatial nodes placed at the vertices of a Yee cube (see figure 2a) there are 8 nodes × 2 fields × 3 components = 48 field components. Only three of these field components are calculated for a given time step. This saves a factor of 16 in computational effort without loss of accuracy. The more naive approach of calculating all components would be equivalent to running 16 Yee schemes in parallel. More accuracy is gained by decreasing step sizes instead of caculating more components.

The three dimensional grid is constructed in such a way that the faces are symmetric and contain two tangential electric field components and one normal magnetic field component. This is illustrated in figure 2b.

## 2.3 Consistency

The method is consistent if the truncation error $\tau_m^n \to 0$ as $h, k \to 0$ for all indexes $n$ and $m$. The truncation error can be obtained by Taylor expanding the components in (4b) and setting $c = 1$,

$$\frac{\partial E_z|_m^{n+\frac{1}{2}}}{\partial t} = \frac{1}{k}\left(E_z|_m^{n+1} - E_z|_m^n\right) + \mathcal{O}(k^2), \tag{7a}$$

$$\frac{\partial B_y|_m^{n+\frac{1}{2}}}{\partial x} = \frac{1}{h}\left(B_y|_{m+\frac{1}{2}}^{n+\frac{1}{2}} - B_y|_{m-\frac{1}{2}}^{n+\frac{1}{2}}\right) + \mathcal{O}(h^2). \tag{7b}$$

Equation (4b) gives that (7a) equals (7b) for $c = 1$. Equating the rigth hand sides of (7) yields

$$E_z|_m^{n+1} = E_z|_m^n + \frac{h}{k}\left(B_y|_{m+\frac{1}{2}}^{n+\frac{1}{2}} - B_y|_{m-\frac{1}{2}}^{n+\frac{1}{2}}\right) + \mathcal{O}(k^3 + kh^2). \tag{8}$$

Hence, the truncation error is

$$k\tau_m^n = \mathcal{O}(k^3 + kh^2), \tag{9}$$

and thus we have consistency.

The same approach can be used to prove consistency in three dimensions. Setting $c = 1$ and using Taylor expansion on the components in (2) as in (7), shows that the update equations for three dimensions (6) also have an truncation error of $\mathcal{O}(k^3 + kh^2)$. The derivation goes along the same lines as above and is left out for brevity's sake.

## 2.4 Numerical stability

The CFL-condition provides a necessary condition for stability. In the one dimensional explicit case the condition can be formulated as

$$\frac{ck}{h} = cp \le 1. \tag{10}$$

In three dimensions the CFL-condition is

$$k\left(\frac{v_x}{\Delta x} + \frac{v_y}{\Delta y} + \frac{v_z}{\Delta z}\right) \le 1. \tag{11}$$

Assuming a uniform discretization grid with stepsize $h$ yields

$$k \cdot 3\frac{c/\sqrt{3}}{h} = \sqrt{3}pc \le 1. \tag{12}$$

This requirement also makes sense intuitively. Having the numerical method move in space can not be done if the information moving in time is not allowed to catch up. The number required to be bounded is known as the Courant number. In order to prove stability of the Yee scheme one needs a *sufficient* condition. In order to allow a more compact notation, the electric and magnetic fields will be represented in one single, complex vector field

$$\mathbf{U}_{i,j,k}^n = \mathbf{B}_{i,j,k}^n + \hat{\imath}\mathbf{E}_{i,j,k}^n, \tag{13}$$

where $\hat{\imath} = \sqrt{-1}$. Now the two first Maxwell equations (1a) and (1b) can be rewritten as one single equation,

$$c\hat{\imath}\nabla \times \mathbf{U} = \frac{\partial \mathbf{U}}{\partial t}. \tag{14}$$

Now we decompose the finite difference-scheme into separate time and space eigenvalue problems,

$$c\hat{\imath}\nabla\times|_{\text{numerical}}\mathbf{U}_{i,j,k}^n = \lambda\mathbf{U}_{i,j,k}^n, \tag{15a}$$

$$\frac{\partial}{\partial t}\Big|_{\text{numerical}}\mathbf{U}_{i,j,k}^n = \lambda\mathbf{U}_{i,j,k}^n. \tag{15b}$$

This decomposition, first proposed by Taflove [1], corresponds to the plane-wave eigenmodes of the EM-wave. We achieve stability if all such wave modes are bounded as time tends to infinity [6]. A stable range for $\lambda$ in (15) will be determined which can guarantee this. Let's first look at the time eigenvalue

**Figure 2**

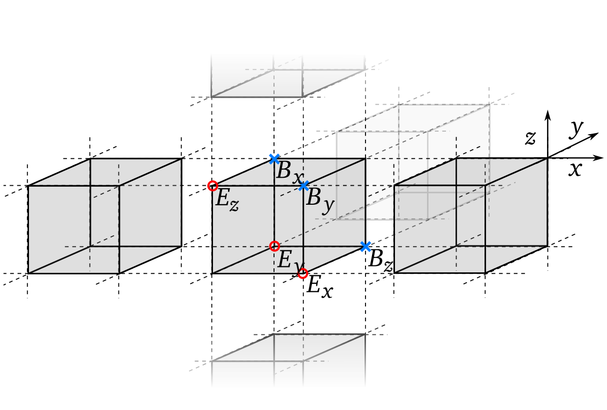


(a) Yee's discretization scheme in three dimensions. Each grey cube is one basic grid unit, where each cube have the same variables calculated in each node as shown on the middle cube. As in one dimension, only one of the fields are present at each time level.

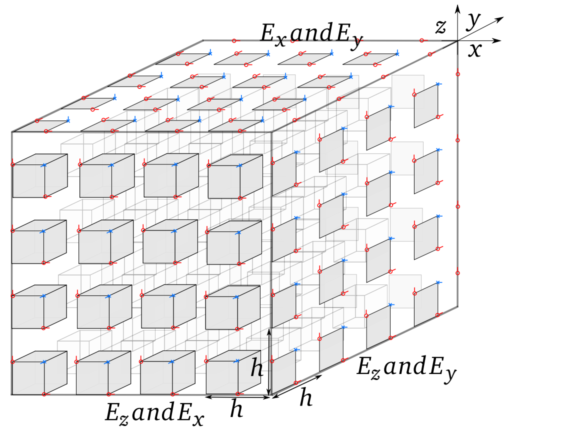


(b) The boundaries of a $(5\times5\times5)$ domain. None of the field components actually has the given dimension. In this case the dimensions are $E_x(4\times5\times5)$, $E_y(5\times4\times5)$, $E_z(5\times5\times4)$, $H_x(5\times4\times4)$, $H_y(4\times5\times4)$ and $H_z(4\times4\times5)$.

problem (15b), inserting our numerical scheme on the left hand side

$$\frac{\mathbf{U}^{n+1/2}_{i,j,k}-\mathbf{U}^{n-1/2}_{i,j,k}}{k}=\lambda\mathbf{U}^n_{i,j,k}. \tag{16}$$

Now define a solution growth factor

$$\xi_{i,j,k}=\frac{\mathbf{U}^{n+1/2}_{i,j,k}}{\mathbf{U}^{n}_{i,j,k}}=\frac{\mathbf{U}^{n}_{i,j,k}}{\mathbf{U}^{n-1/2}_{i,j,k}}. \tag{17}$$

Inserting (17) into (16) and solving the quadratic equation for $\xi_{i,j,k}$ gives

$$\xi_{i,j,k}=a\pm\sqrt{a^2+1},\quad \text{where } a=\frac{\lambda k}{2} \tag{18}$$

Now we require $|\xi_{i,j,k}|\le 1$ for *all* possible modes in the grid $(i,j,k)$. This is satisfied when $a$ is purely imaginary and bounded between $-\hat{\imath}$ and $\hat{\imath}$, which imposes the following stability constraint on the eigenvalues

$$-\frac{2\hat{\imath}}{k}\le\lambda\le\frac{2\hat{\imath}}{k}. \tag{19}$$

Now let's analyse the space eigenvalue problem (15a) using von Neumann stability analysis. Apply a Fourier-transform to an instantaneous time step $n$ of the spatial grid to provide an alternative representation,

$$\mathbf{U}^n_{i,j,k}=\mathbf{U}_0e^{\hat{\imath}h(\beta_x i+\beta_y j+\beta_z k)}. \tag{20}$$

Using the central differences from the Yee scheme to approximate the spatial derivatives of the curl operator, one can rewrite (15a) as

$$-\frac{2c}{h}\Big[\sin(\beta_x h/2),\sin(\beta_y h/2),\sin(\beta_z h/2)\Big]^{\mathsf{T}} \times\mathbf{U}^n_{i,j,k}=\lambda\mathbf{U}^n_{i,j,k}. \tag{21}$$

The sinusoidal terms arise from the application of Euler's identity. Performing the cross product yields a system of three equations which then is solved for $\lambda$

$$\lambda=-\frac{2ci}{h}\sqrt{\sin^2(\beta_x h/2)+\sin^2(\beta_y h/2)+\sin^2(\beta_z h/2)}. \tag{22}$$

For all $\beta_x$, $\beta_y$, and $\beta_z$ we have that

$$-\frac{\sqrt{3}\hat{\imath}}{h}\le\lambda\le\frac{\sqrt{3}\hat{\imath}}{h}. \tag{23}$$

In order to still *guarantee* $|\xi_{i,j,k}|\le1$, i.e. numerical stability for an arbitrary spatial mode, the radius of the spatial eigenvalues (23) needs to be contained completely within the range of temporal eigenvalues (19) [6]. This gives an upper bound on the time step

$$k\le\frac{h}{\sqrt{3}c}. \tag{24}$$

The necessary CFL stability criterion is therefore also a sufficient one. Combined with numerical consistency this implies convergence, according to the Lax' equivalence theorem [4].

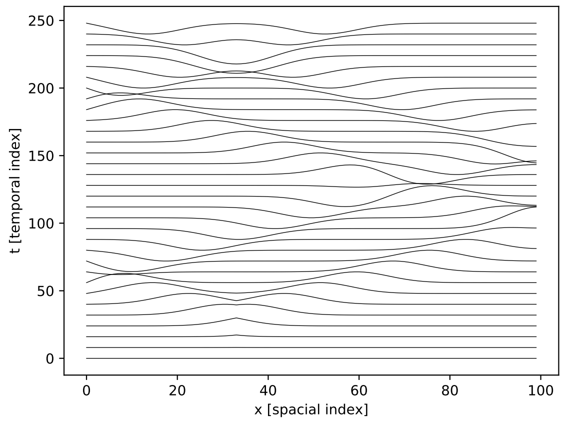


**(a)** Pulse initialized by additive source in spacial index 33. Perfect conductors as boundaries. Additive source: Ez[33] += $\exp(-(t-30)^2/100)$.

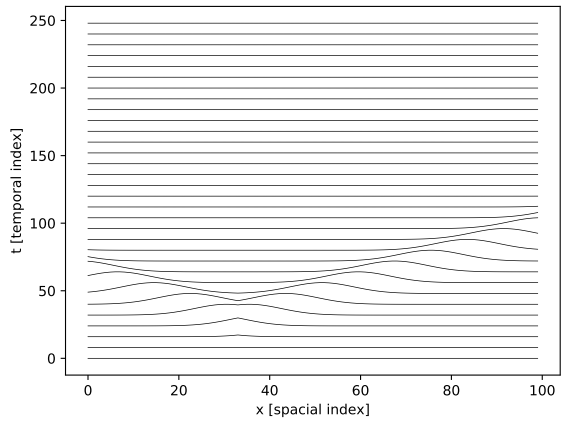


**(b)** Pulse initialized by additive source in spatial index 33. Absorbing boundary conditions. Additive source: Ez[33] += $\exp(-(t-30)^2/100)$.

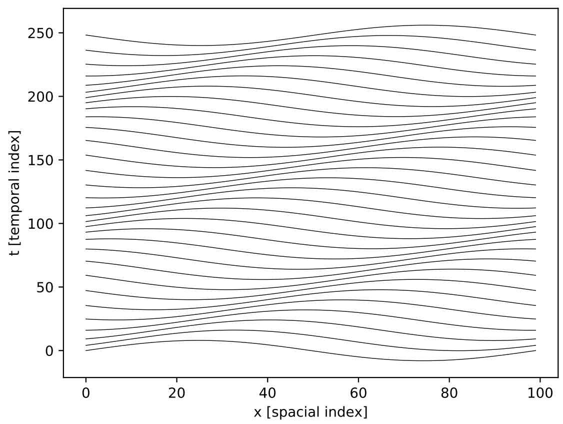


**(c)** Infinite sinusoidal wave obtained by use of periodic boundary conditions. Initial conditions: $E_z = \sin(2\pi x), \quad B_y = -\sin(2\pi x)$.

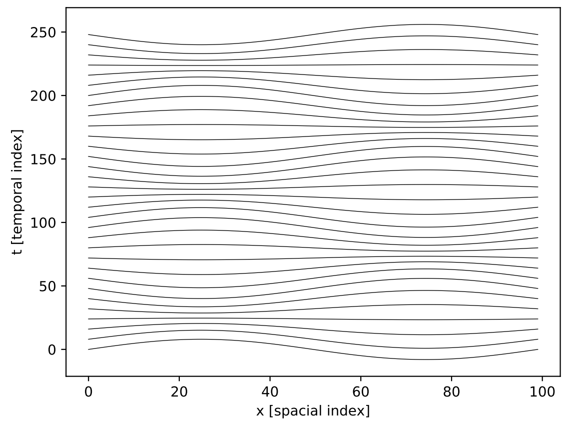


**(d)** Standing wave obtained by setting initial magnetic field to zero and use of periodic boundary conditions. Initial conditions: $E_z = \sin(2\pi x), \quad B_y = 0$.

**Figure 3:** Waterfall plots of electric field using an additive source or specific initial conditions and different boundary conditions.

## Numerical Experiments

The method described in (5) is used to approximate solutions to problems with given initial conditions and boundary conditions in one dimension. Solutions corresponding to a selection of different initial conditions and boundary conditions are displayed by use of waterfall plots in figure 3.

The update equations in (6) are used to obtain solutions for different initial and boundary conditions in three dimensions. Plots showing the results are displayed in figure 4 as slices, and in figure 5 as snapshots. The slices can be thought of as planes slicing the domain in the middle of the considered $z$ - interval.

The sinusoidal wave in figure 4a is a numerical solution that is well-behaved and closely resembles the analytical solution. This problem doesn't seem to possess properties that makes the numerical method behave in an irregular way. It is therefore used to obtain convergence plots. The sinusoidal wave portrayed in figure 4b and 5a is not traveling along one axis exclusively and shows some clear deviation from the analytical solution. The numerical artifacts observable when simulating waves traveling diagonally relative to the Yee cubes (and by proxy, also the coordinate axes) have been noted by Taflove [6], among others.

If we set the variations in $y$- and $z$-direction to be zero for the Maxwell relations (1), we obtain that the electric field $E_z$ can be expressed in the form of the one-dimensional wave equation. The solution to this equation can be easily found and is commonly known as d'Alembert's solution. An analytical solution is therefore available for any given set of initial conditions. This leaves us with a reference solution which can be used to assert the correctness of the numerical method in one dimension.

In three dimensions the Maxwell relations can be used to express the electric field as the solution to a three dimensional vector wave equation, but finding a solution satisfying this equation for arbitrary initial conditions is not done easily. A more convenient approach for obtaining a three-dimensional reference solution is simply to "extend" the easily obtainable one-dimensional solution to three dimensions. This leaves us with a planar, three-dimensional wave. The analytical solution for such a wave can be used as a reference solution when investigating the order of convergence for the method in three dimensions. The resulting convergence plots indicate that the method is of order 2 in space for both one and three dimensions. The convergence is displayed in figure 6a and 6b. These plots are obtained by comparing the numerical results to the reference solution. The results are in line with what one would expect from looking at the theoretical global truncation error of the method.

The approach of using an analytical solution as a reference solution works well when considering convergence in space, but problems arise when attempting to confirm the expected convergence in time with the same approach. The method doesn't seem to improve much relative to the analytical solution when decreasing the stepsize in time. This seems to be caused by a combination of two factors. Firstly, varying degrees of dispersion, and secondly, increasing deviation from the optimal value of the stepsize ratio, $\sqrt{3}pc$. The optimal value has been shown to be equal to one in the literature [5]. This is hard to maintain when constructing a convergence plot. With regards to dispersion, it has been seen to occur in cases where the solution is a sinusoidal wave, which is the case for the problem used when exploring the convergence of the method. Methods for dealing with dispersion is discussed in the literature [5], but has not been prioritized in our implementation.

The problem of not being able to observe convergence when an analytical solution is used as the reference solution is partly solved by creating a reference solution from running the numerical method with very small stepsizes in time. The resulting convergence plots, shown in figure 6a and 6b indicate that the method is of order 1. This is not in line with what is expected as the global truncation error is expected to be $\mathcal{O}(h^2 + k^2)$.

## Conclusion

The numerical method known as the "Yee method" is shown to generate a solution in a number of different

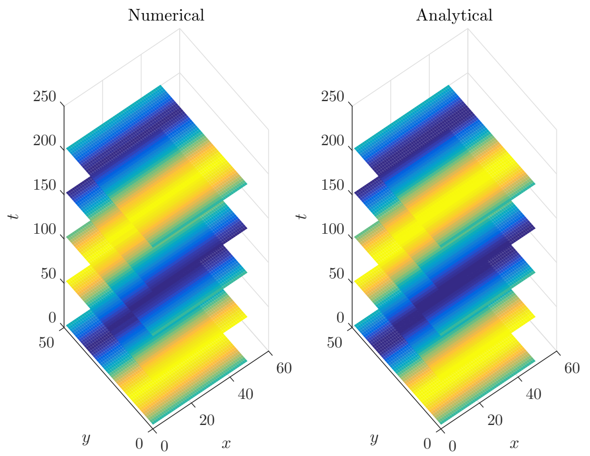


**(a)** Numerical and analytical solution with periodic boundary conditions and initial condition $\mathbf{E} = (0, 0, \sin(2\pi x)), \mathbf{B} = (0, -\sin(2\pi x), 0)$. The analytical solution is $E_z = \sin(2\pi(x + ct))$.

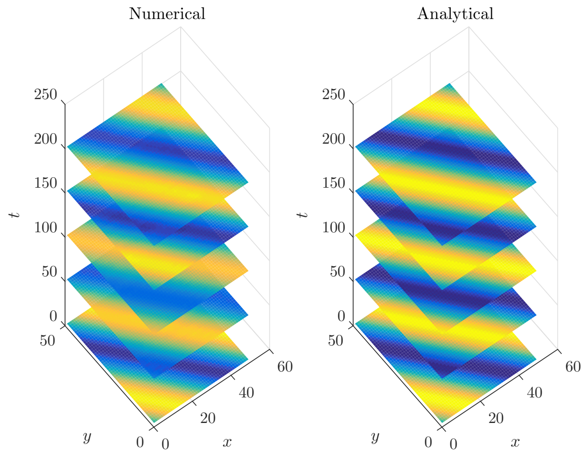


**(b)** Numerical and analytical solution with periodic boundary conditions and initial condition $E_z = \sin(2\pi(x + y)), B_y = -\sin(2\pi(x + y))$. The analytical solution is $E_z = \sin(2\pi(x + y - \sqrt{2}ct))$.

**Figure 4:** Slice plots of solutions in 3D. The colors indicate the amplitude of the $E_z$-field at the given time and position. The numbers on the $x$- and $y$-axis denotes the grid index, and the numbers on the $t$-axis denotes the time step.

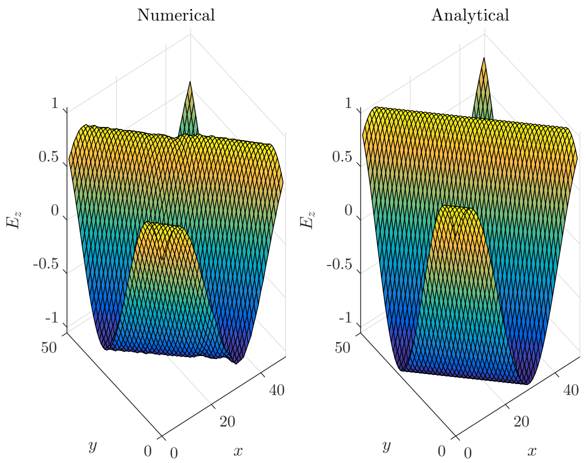


**(a)** Numerical and analytical solution with periodic boundary conditions at time $t = 1/5c$ and initial condition $\mathbf{E} = (0, 0, \sin(2\pi(x + y))), \mathbf{B} = (0, -\sin(2\pi(x + y)), 0)$. The analytical solution is $E_z = \sin(2\pi(x + y - \sqrt{2}ct))$.

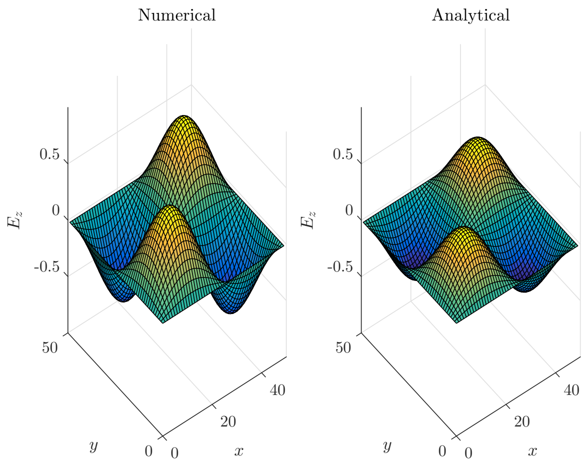


**(b)** Numerical and analytical solution with periodic boundary conditions at time $t = 3/5c$ and initial condition $\mathbf{E} = (0, 0, \sin(2\pi x)\sin(2\pi y)), \mathbf{B} = (0, 0, 0)$. The analytical solution is $E_z = \cos(8\pi ct)\sin(2\pi x)\sin(2\pi y)$

**Figure 5:** Snapshots of numerical and analytical solutions. The $x$- and $y$-axis denotes the grid indexes and the $z$-axis denotes the amplitude of the $E_z$-field at the given position and time.

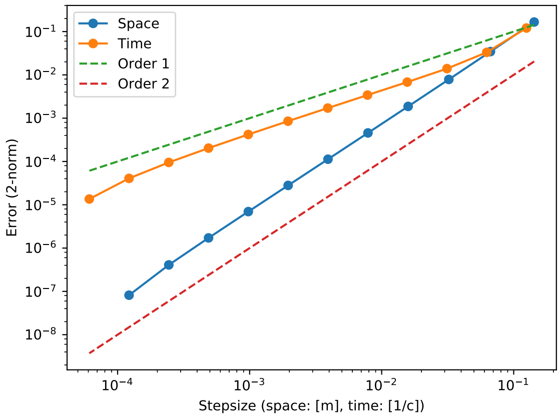


**(a)** Convergence plot for the Yee method in one dimension, with $E_z(x) = \sin(2\pi(x - ct))$. The space between $x_0 = 0$ and $x_N = 1$ is considered, with time fixed at $t = 1/c$

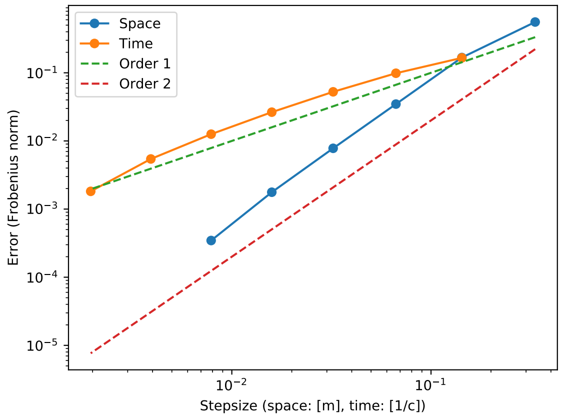


**(b)** Convergence plot for the Yee method in three dimensions with $E_z = \sin(2\pi(x - ct))$. The spatial coordinates are restricted to values between 0 and 1 with time fixed at $t = 1/c$.

cases and the associated convergence plots points to a steady decrease in error. The order of convergence in space is shown to be of order 2, which is in accordance with the theory. The method fails to agree with theory when considering the order of convergence in time. The theory suggest that the convergence should be of order 2, but plots indicate that the order is 1. A definite explanation to this problem has not been found and warrants further exploration. Restrictions on the number of temporal nodes relative to the number of spatial nodes, imposed by the CFL-condition, makes the problem hard to investigate as thoroughly as desired. Possible explanations could be things such as decreasing and sub-optimal Courant number and unexpected implications on time-convergence caused by the number of spatial steps. Dispersion has also been observed in some cases, which further complicates the problem. Despite these issues, the method displays good behaviour in a variety of situations, and closely the mimics either the analytical solution or the numerical reference solution when small enough stepsizes are used.

## References


[1] A. T. . M. E. Brodwin, *Numerical solution of steady-state electromagnetic scattering problems using the time-dependent maxwell's equations*, (1975).

[2] L. Changli, *Comments on overdetermination of maxwell's equations*. https://arxiv.org/pdf/1002.0892.pdf, September 2016.

[3] R. G. Littlejohn, *Gaussian, SI and other systems of units in electromagnetic theory*. http://bohr.physics.berkeley.edu/classes/221/1112/notes/emunits.pdf, 2016.

[4] B. Owren, *TMA4212 Numerical solution of partial differential equations with finite difference methods*, NTNU, 2014.

[5] J. B. Schneider, *Understanding the finite-difference time-domain method*. http://www.eecs.wsu.edu/~schneidj/ufdtd/ufdtd.pdf, April 2016.

[6] A. Taflove, *Computational Electrodynamics: The Finite-Difference Time-Domain Method*, Artech House, Inc., 1995.

[7] K. Yee, *Numerical solution of initial boundary value problems involving maxwell's equations in isotropic media*, (1966).